Protonation Dynamics of the α-Toxin Ion Channel from Spectral Analysis of pH-Dependent Current Fluctuations

John J. Kasianowicz* and Sergey M. Bezrukov‡§

*National Institute of Standards and Technology, Biotechnology Division, Biosensors Group, Gaithersburg, Maryland 20899 USA; ‡National Institutes of Health, Laboratory of Structural Biology, Bethesda, Maryland 20892 USA; and §St. Petersburg Nuclear Physics Institute of the Russian Academy of Sciences, Gatchina, Russia 188350

ABSTRACT To probe protonation dynamics inside the fully open α-toxin ion channel, we measured the pH-dependent fluctuations in its current. In the presence of 1 M NaCl dissolved in H_2O and positive applied potentials (from the side of protein addition), the low frequency noise exhibited a single well defined peak between pH 4.5 and 7.5. A simple model in which the current is assumed to change by equal amounts upon the reversible protonation of each of N identical ionizable residues inside the channel describes the data well. These results, and the frequency dependence of the spectral density at higher frequencies, allow us to evaluate the effective pK = 5.5, as well as the rate constants for the reversible protonation reactions: $k_{on} = 8 \times 10^9\ M^{-1}\ s^{-1}$ and $k_{off} = 2.5 \times 10^4\ s^{-1}$. The estimate of k_{on} is only slightly less than the diffusion-limited values measured by others for protonation reactions for free carboxyl or imidazole residues. Substitution of H_2O by D_2O caused a 3.8-fold decrease in the dissociation rate constant and shifted the pK to 6.0. The decrease in the ionization rate constants caused by H_2O/D_2O substitution permitted the reliable measurement of the characteristic relaxation time over a wide range of D^+ concentrations and voltages. The dependence of the relaxation time on D^+ concentration strongly supports the first order reaction model. The voltage dependence of the low frequency spectral density suggests that the protonation dynamics are virtually insensitive to the applied potential while the rate-limiting barriers for NaCl transport are voltage dependent. The number of ionizable residues deduced from experiments in H_2O (N = 4.2) and D_2O (N = 4.1) is in good agreement.

INTRODUCTION

Ion channels are membrane-bound proteins that enable cells to communicate with each other, to sense ligands, and to maintain their homeostasis. By virtue of their small size and their ability to span an electrically insulating lipid bilayer that separates two regions of bulk fluid, channels also provide the means to study the dynamics of chemical reactions that might occur in a highly confined region. In this sense, ion channels can be likened to nanoscale test tubes in which reaction dynamics are probed by analyzing the frequency content of the current fluctuations. We report here the use of an ion channel to study rapid protonation reactions that take place in its lumen.

Proton transport adjacent to and through membranes and proteins is of fundamental significance in bioenergetics (Mitchell, 1961). However, the dynamic character of proton movement in these environs has been the subject of intense debate in recent years. There is still a need for experimental methods to distinguish between highly disparate models for proton transport in similar systems. We propose here that ion channels might be useful to study fast chemical reactions associated with ionization and proton transport that occur adjacent to biological interfaces. For detailed discussions on proton movement near the surfaces of lipids and proteins, we refer the interested reader to several reviews (Deamer and Nicholls, 1989; Gutman and Nachliel, 1990; Deamer, 1992; Heberle et al., 1994).

In this study, we address the question of how rapidly protons move in the confines of an open ion channel by studying the dynamics of ionization reactions that alter the conducting properties of the channel formed by *Staphylococcus aureus* α-toxin. The rate constants for proton association and dissociation with specific amino acids that line the channel lumen are deduced by characterizing the pH dependence of both the open channel current-voltage relationship and its current noise.

The analysis of fluctuations in a physical observable has been used to describe successfully the properties of a wide variety of systems and to determine the value of several fundamental physical constants. For example, measurements of the shot noise in vacuum tubes were used to estimate the electron charge (Schottky, 1918). In some physical systems, equilibrium, kT-driven fluctuations cause phenomena that are easily observed without instrumentation. In particular, density fluctuations of a non-ideal gas at its critical point can cause light scattering (critical opalescence) that is easily visualized with the unaided eye (Stanley, 1971). Interesting and detailed discussions on stochastic methods and random processes in physical and chemical systems are found in several excellent textbooks (e.g., Gardiner, 1985; van Kampen, 1981; Wax, 1954).

Noise analysis played an important role in postulating the existence of protein ion channels. Measurements of the noise spectra performed on biological membranes of differ-

Received for publication 30 November 1994 and in final form 14 April 1995.

Address reprint requests to Dr. John J. Kasianowicz, Biotechnology Division, National Institute of Standards and Technology, Bldg. 222, Rm. A353, Gaithersburg, MD 20899. Tel.: 301-975-5853; Fax: 301-330-3447; E-mail: jkasianowicz@enh.nist.gov.

0006-3495/95/07/94/12 $2.00

ent origin (see reviews by Stevens, 1977; DeFelice, 1981; Neumcke, 1982; Fishman and Leuchtag, 1990) gave support to the pore hypothesis showing that the current flowing through an individual channel is $\sim 10^7$ ions/s (Hille, 1992).

The ability to reconstitute single channels into planar bilayers (Bean et al., 1969) and the development of the single channel recording technique (Neher and Sakmann, 1976) opened new possibilities for studying the interaction of chemical compounds (e.g., neurotransmitters, neurotoxins, and anesthetics) with a channel, since the analyte would either block the pore or elicit a change in the gating properties of the channel. However, even in the absence of channel-modifying agents, the current through unperturbed ion channels also exhibits noise and yields information about ion transport properties of these structures (Sigworth, 1985; Heinemann and Sigworth, 1991).

We studied open channel noise in the pore formed by α-toxin, one of several protein exotoxins secreted by *S. aureus* (Thelestam and Blomqvist, 1988). As a 33.1-kDa molecular weight monomer it is water soluble, yet spontaneously forms large pores in biological membranes (Bhakdi and Tranum-Jensen, 1991), lipid vesicles (Ikigai and Nakae, 1987), and planar bilayer membranes (Menestrina, 1986). Experimental evidence suggests that the channel is a homooligomer (Gouaux et al., 1994) with an internal diameter between 1.1 and 2.5 nm (Füssle et al., 1981; Bhakdi et al., 1984; Menestrina, 1986; Krasilnikov et al., 1992). The primary sequence of the protein is known (Gray and Kehoe, 1984; Walker et al. 1992), and a recombinant version of the molecule has been produced in *S. aureus* (Palmer et al., 1993), in *Escherichia coli* (Walker et al., 1992), and in an in vitro transcription and translation system (Walker et al., 1992). A suite of genetically engineered mutants of α-toxin has been produced and is now shedding light on the mechanism of channel assembly (Walker and Bayley, 1994).

We measured the fluctuations in current through fully open α-toxin channels reconstituted into planar lipid bilayer membranes. A short report, which was restricted to experiments with H_2O electrolyte solutions and mainly addressed the dependence of low frequency protonation noise on pH, was published earlier (Bezrukov and Kasianowicz, 1993). In the present study, we describe the changes in protonation noise that occur with solvent substitution (H_2O/D_2O) and show that a decrease in the reaction rates correlates with the decrease in mobility of D^+ compared with that of H^+. In addition, the variation of current noise with applied potential demonstrates that the ionization-dependent rate constants of electrolyte transport through the channel are voltage sensitive while the ionization dynamics themselves are not. Finally, the pD ($-\log_{10}(a_{D+})$) dependence of the protonation relaxation time shows that the ionization process is consistent with a first order reaction scheme.

MATERIALS AND METHODS

We used the following reagents: "purum" hexadecane (Fluka, Buchs, Switzerland), diphytanoyl phosphatidylcholine (Avanti Polar Lipids, Inc., Alabaster, AL), high purity pentane (Burdick and Jackson, Muskegon, MI), NaCl (Mallinckrodt, St. Louis, MO), citric acid (J. T. Baker, Phillipsburg, PA), Tris and agarose (Bethesda Research Laboratory, Gaithersburg, MD), ultrol grade MES or HEPES (Calbiochem, San Diego, CA), and TAPS and D_2O (Sigma Chemical Co., St. Louis, MO). The water was purified by a Hydro deionization system (Research Triangle Park, NC) and bidistilled in a quartz apparatus (Heraues-Schott, Mainz, Germany).

Solvent-free planar lipid bilayer membranes were formed from diphytanoyl phosphatidylcholine in pentane on a 50 μm diameter orifice in a 15 μm thick Teflon partition that separated two chambers (after Montal and Mueller, 1972). The orifice was pretreated with a 10% solution of hexadecane in pentane (v/v). Unless otherwise specified, the aqueous solutions were prepared with 1 M NaCl, 2.5 mM MES or HEPES either in purified H_2O or in D_2O, $T = (24.0 \pm 1.5)$°C.

The activity of deuterium ion, and thus pD, was estimated using a glass pH electrode that was calibrated with pH standard buffers. It is known that the pH-sensitive glass electrode response is Nernstian in D_2O solutions, but there is an offset compared with similar acid concentrations in H_2O, such that pD = pH + 0.4, where pH is the reading of the electrode in a deuterium aqueous solution (Glasoe and Long, 1960; Covington et al., 1968; Bates, 1973).

Single channels were formed in the presence of symmetric solutions by adding <1 μg *S. aureus* α-toxin to 1.5 ml of aqueous solution in the *CIS* chamber while stirring. The time that elapsed between the addition of protein to the membrane bathing solution and the appearance of a single channel varied depending upon the solution pH (pD). Specifically, lower values of pH corresponded to shorter insertion times. We adjusted the protein concentration to obtain a single channel within 10 min. We occasionally observed channels with a conductance that was about one-half of the mean value for the particular solution. We excluded these events in our analysis.

The electrical potential difference across the bilayer was applied with Ag-AgCl electrodes in 3 M KCl, 1.5% agarose bridges. The applied potential is defined as positive when it is greater at the side of protein addition (*CIS*). The current was amplified by a Dagan 3900 patch-clamp amplifier (Minneapolis, MN) in the mixed RC mode with a 3901 or 3902 headstage, digitized by a Toshiba/Unitrade PCM recorder (Philadelphia, PA) onto VHS tape and subsequently transferred to a personal computer through a Frequency Devices eight-pole Butterworth filter (Haverhill, MA), the corner frequency of which was set to 3/8 of the sampling frequency of either an ADALAB A/D board (State College, PA) or a National Instruments AT-MIO-16X A/D board (Austin, TX). The spectral density was determined by using a Fast Fourier Transform on 2048 point vectors. The membrane chamber, headstage, and source of the applied potential were isolated from external electrical and magnetic noise sources by a shield fabricated from mu-metal (Amuneal Corp., PA).(Commercial names of materials and apparatus are identified only to specify the experimental procedure. This does not imply a recommendation, nor does it imply that they are the best available for the purpose.)

RESULTS AND MODEL

Since the primary sequence of the α-toxin monomer contains 96 ionizable amino acids (Gray and Kehoe, 1984; Walker et al., 1992), it is hardly surprising that several properties of the α-toxin ion channel are altered by pH changes. For example, typical single channel current recordings over long time periods illustrated in Fig. 1 show that the probability of the channel gating to closed states in a given time interval decreases when the pH is increased from 4.5 to 7.5. However, we choose here to ignore the pH sensitivity of the gating dynamics of this channel and restrict ourselves to the changes in current that occur over much shorter time scales for which the channel does not gate and remains in the fully open conformation.

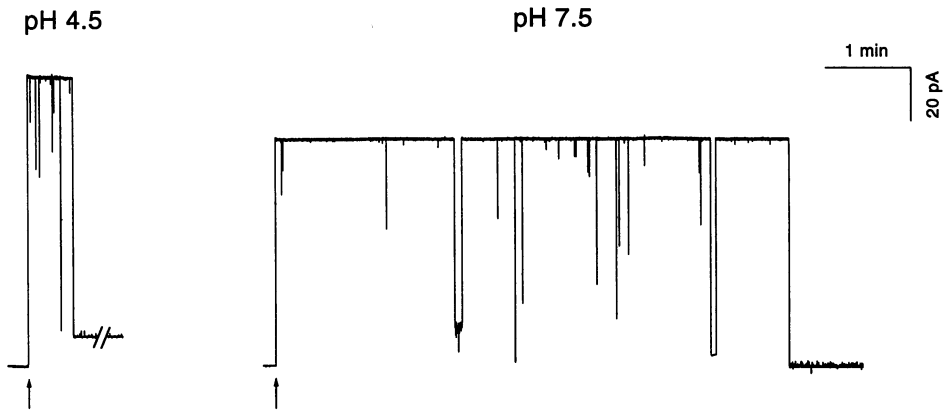

FIGURE 1 Typical single channel current recordings in the presence of *S. aureus* α-toxin on the time scale of several min. The arrows indicate the application of +140 mV across the membrane, which causes a current of ~100 pA to flow. Note that the channels switch or gate between open and different partially closed states until they access a closed state from which they virtually never recover, unless the potential is reduced. The gating behavior depends on the pH of the bathing solution. Higher pH corresponds to a greater open state lifetime. These particular recordings illustrate that at higher pH, the channel stays open ~10 times longer than that at the lower pH value. The aqueous (H_2O) solutions contained 1 M NaCl and 2.5 mM MES (pH 4.5), or 1 M NaCl, 2.5 mM MES and 2.5 mM TAPS (pH 7.5). The signals were filtered at 30 Hz.

The current recordings shown in Fig. 2 *A* illustrate the formation of single channels, in the presence of H_2O aqueous solutions, for three different pH values at time scales of several seconds. Note that the current varies with pH in two ways. Not only does the mean current decrease when the pH is increased from pH 4.6 to 7.55, but there is a marked difference in the characteristic noise of the open state of the channel at the three different pH values. The noise track, corresponding to the current through the channel at pH 5.9 is wider compared with those at pH 4.6 and 7.55. The single channel recordings contain background noise from the electrodes and electronics. Nevertheless, the non-monotonic behavior of the noise generated by the channel itself is clearly evident.

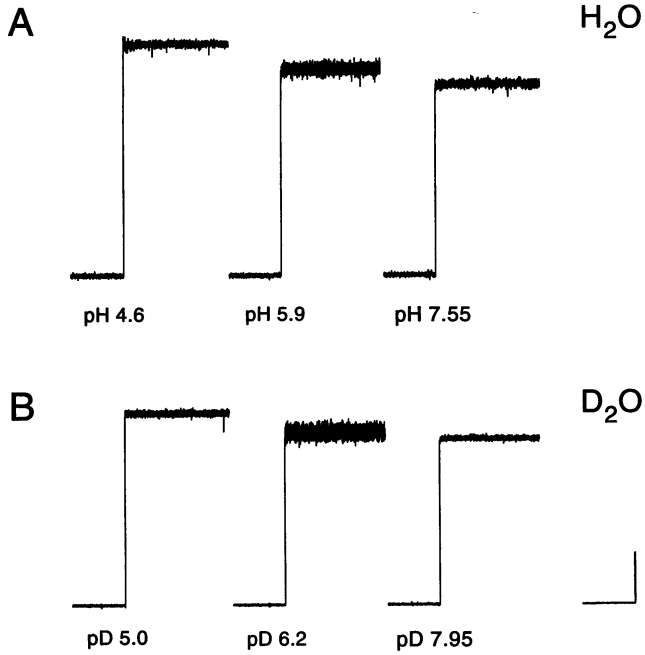

FIGURE 2 Single channel current recordings of α-toxin on the time scale of several seconds. The rapid change in current corresponds to the spontaneous insertion of a single channel in solutions with three different pH (or pD) values and either H_2O (*A*) or D_2O (*B*) as a solvent. Note that the current decreases monotonically with increasing pH (pD) but the current noise rises at intermediate pH values. The solutions contained 1 M NaCl and 2.5 mM of a proton buffer (see Materials and Methods). The applied potential was +150 mV. The current and time scales indicate 25 pA and 1 s, respectively. The signals were filtered at 1 kHz.

Fig. 2 *B* shows that solvent substitution of D_2O for H_2O causes distinct changes in the channel current. The decrease in the ionic current carried by NaCl in D_2O is reasonably consistent with the increased viscosity of D_2O compared with H_2O (Kirshenbaum, 1951; Heiks et al., 1954; Swain and Evans, 1966). However, comparison of the recordings in Fig. 2, *A* and *B*, shows that the pH (pD)-dependent noise effect persists. Solvent-induced effects will be discussed in detail later in this paper.

The pH dependence of the mean current and current noise can be understood in terms of a simple model, which is presented in Fig. 3. As we proposed earlier (Bezrukov and Kasianowicz, 1993), we consider the reversible binding of protons to ionizable residues inside the channel to be the basis for the observed changes in the channel mean current and noise (Figs. 2, *A* and *B*). Specifically, the binding of a proton to a single residue induces a change in the electrostatic potential profile in the channel, causing a stepwise increase in the current carried by the electrolyte, in this case NaCl. In general, there may be several different types of such sites. However, for the sake of simplicity, we assume here that the pK values of the ionizable groups are identical, that the binding of a proton to each of these sites has the same effect on the channel current, and that the probability of a proton binding to a site is independent of the state of the other $N - 1$ such sites (see Discussion).

The model describes well the non-monotonic behavior of the current noise. Indeed, for pH values much less than the

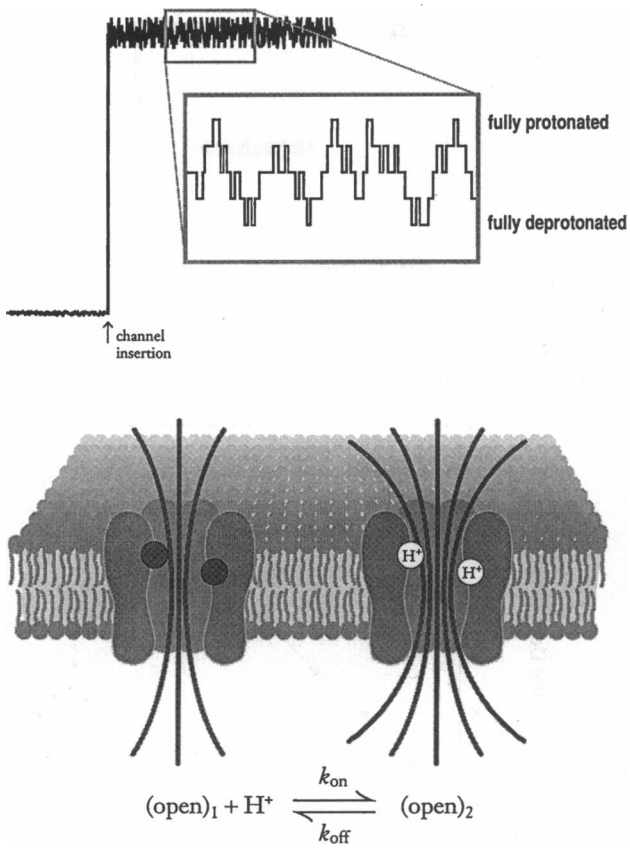

FIGURE 3 An illustration of the model for protonation reactions. The fluctuations in the current are caused by the modulation of conductance by the reversible ionization of N identical residues inside the channel. According to the model, the charge state of the residues controls the potential barrier for permeant ions (e.g., Na^+ and Cl^-); the protonation of each residue in the pore increases the current by an identical amount. The association and dissociation rate constants are k_{on} and k_{off}, respectively. Only two of the N ionizable residues and only one of the N reaction equations are shown for visual clarity.

pK, the proton concentration is sufficiently high that the ionizable residues are virtually always occupied and the current is at its maximum value. On the other hand, for pH values much greater than the pK, the proton concentration is low enough for the residues to be unoccupied most of the time, which results in the minimum current for a particular voltage. In both cases, the current noise, which is caused by the switching of the channel conductance between different levels, is low. However, for intermediate pH values (pH ~ pK), the residues fluctuate with virtually equal probability back and forth between the two states of protonation, causing maximum current noise. (The maximum low frequency spectral density occurs at $[H^+] = 2K$ or pH ~ pK + 0.3; see Eq. 10.)

Spectral analysis of the current fluctuations permits the separation of contributions from different noise sources (Stevens, 1977; DeFelice, 1981). It decomposes the mean square value of current fluctuations into components at different frequencies providing a description of the noise in terms of its spectral density. One useful property of this description is that spectral densities from parallel independent noise sources add without interference.

The simple model in Fig. 3 makes specific predictions regarding the dynamics of current fluctuations. Thus, we expect simple relaxation spectra for current noise. In particular, if we assume that the ionization dynamics of a single site are described by a two-state Markov process, we would expect a Lorentzian spectrum of the form

$$S(f) = \frac{S(0)}{1 + (2\pi f\tau)^2}, \quad (1)$$

where $S(f)$ is the current spectral density (in A^2/Hz), f is the frequency (in Hz) and τ is the relaxation time constant (or correlation time) of the system (in s). $S(0)$ is the current spectral density at zero frequency.

The measurement of the spectral density at pH ~ 6 revealed values significantly larger than the shot-noise anticipated for these currents (Heinemann and Sigworth, 1991). Fig. 4 *A* illustrates this for the open channel current of 1.0×10^{-10} A at pH 5.9 (Fig. 4 *A*, *top trace*). The measured noise is two orders of magnitude in excess of the calculated shot noise (~3.2×10^{-29} A^2/Hz) and Johnson noise of the channel (~1.0×10^{-29} A^2/Hz) and dominates at frequencies of 20–2000 Hz over the background (Fig. 4

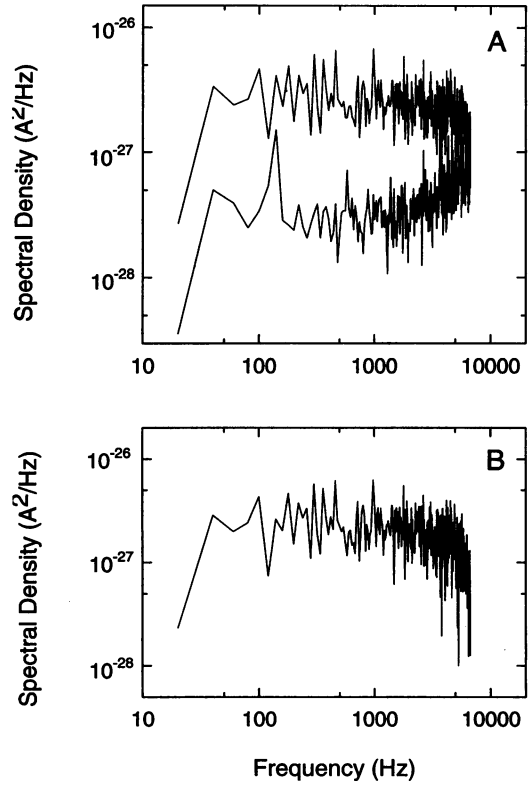

FIGURE 4 (*A*) *Top trace*: the current spectral density of a single α-toxin channel in 1 M NaCl in H_2O, pH 5.8; *bottom trace*: background spectrum taken immediately before the spontaneous insertion of a single channel. (*B*) The difference spectrum showing that the spectral density is constant at low frequencies and decreases at higher frequencies. The applied potential was +150 mV.

A, bottom trace). The difference spectrum presented in Fig. 4 *B* shows a characteristic Lorentzian shape (Eq. 1) for which the spectrum is flat at low frequencies and decays as $1/f^2$ at higher frequencies. Similar results were obtained with D_2O (Fig. 5, *A* and *B*). Note that the corner frequency is decreased by a factor of ~3 by D_2O/H_2O substitution.

In our model, protonation-induced current fluctuations are generated in a single ion channel. Thus, the current noise from simultaneously open channels should be additive. The current record in Fig. 6 *A* illustrates the successive insertion of three channels. Note that the noise increases with the number of open channels. It is easy to discern that the amplitude of the noise is proportional to the square root of the number of channels, as expected for the superposition of random signals from identical, uncorrelated sources. Indeed, our measurements show that the low frequency spectral density is directly proportional to the number of channels (Fig. 6 *B*).

To quantitate the dependence of noise on pH for single channels (Fig. 2), we first analyzed the low frequency portion of the spectra. The magnitude of noise at +150 mV applied potential averaged in the bandwidth of 200–2000 Hz (H_2O; Fig. 7, *filled circles*) and 40–400 Hz (D_2O; Fig. 7, *open circles*) with the background subtracted is illustrated in Fig. 7. Note that there is a pronounced and clearly defined peak in both cases. The noise from the open channel at pH ~ 6 exceeded that of the background by more than an order of magnitude, whereas at the extremes of pH, it was approximately equal to the background.

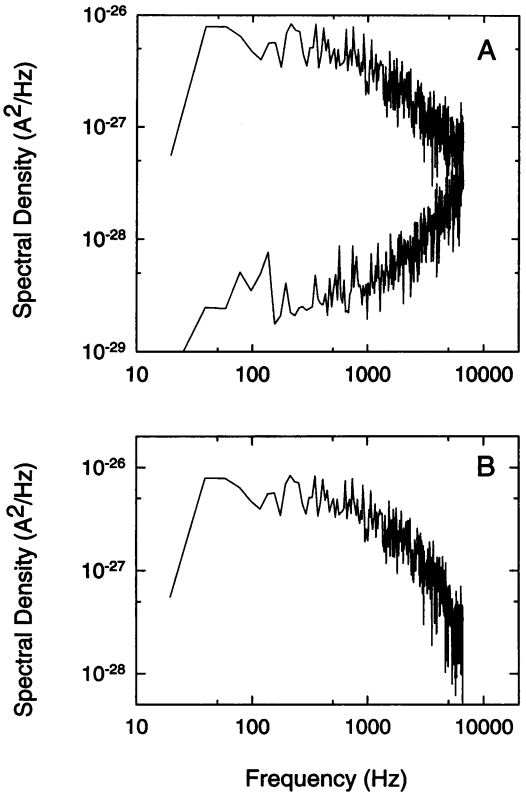

FIGURE 5 (*A*) *Top trace*: the current spectral density of a single α-toxin channel in 1 M NaCl in D_2O, pD = 6.2; *bottom trace*: background spectrum taken immediately before spontaneous channel insertion. (*B*) Note that the difference spectrum is shifted to lower frequencies and greater magnitudes (compared with that for H_2O, Fig. 4 *B*) and shows a characteristic Lorentzian lineshape indicating a simple relaxation process. The transmembrane potential was +150 mV.

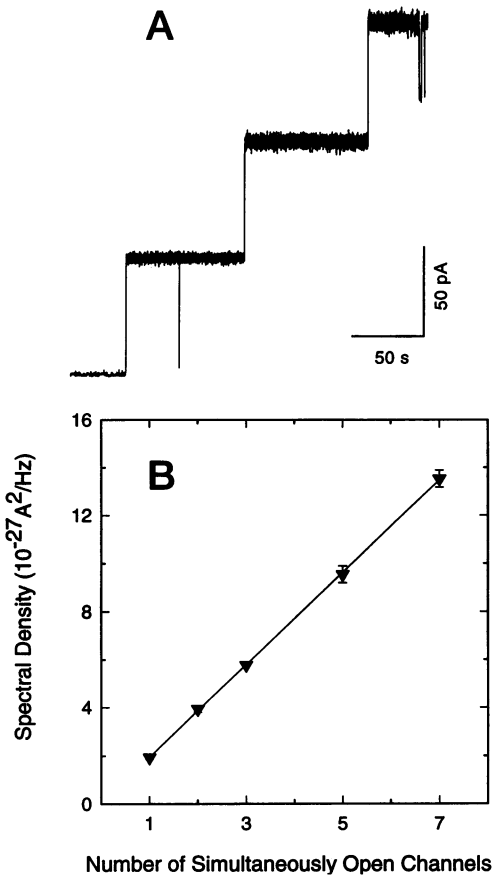

FIGURE 6 The current noise from several channels is additive. (*A*) The current recordings show the successive, spontaneous formation of three channels. The width of the noise track clearly increases with the number of channels. (*B*) The low frequency spectral density is directly proportional to the number of open channels, as expected for channels acting as independent noise sources. The solution contained 1 M NaCl in D_2O, pD = 6.2. The applied potential was +100 mV.

The model illustrated in Fig. 3, which is based on first order reversible ionization reactions, accounts for our results. The effect of pH on the current noise spectral density and conductance of an open α-toxin channel can be described by assuming that an amino acid residue inside the pore can access two distinct states of ionization:

$$A + H^+ \underset{k_{off}}{\overset{k_{on}}{\rightleftharpoons}} H^+A, \qquad (2)$$

where *A* is an ionizable amino acid, and k_{on} and k_{off} are the rate constants for the forward and reverse protonation reactions, respectively. According to the model, the non-ionized state of the residue A, corresponds to a lower conductance state of the

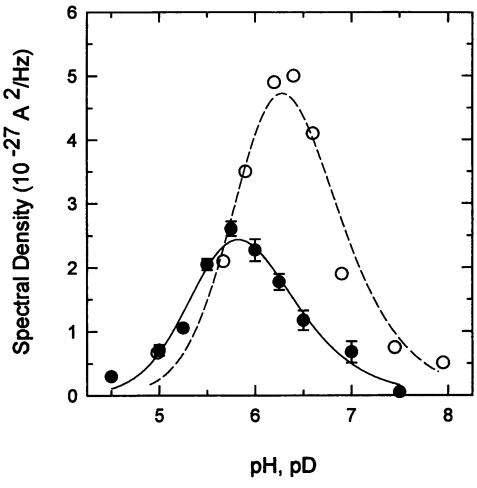

FIGURE 7 The pH (pD) dependence of the low frequency spectral density for H_2O (●) and D_2O (○). The lines are the results of a least-squares fit of Eq. 10 to the data. The H_2O data are well described by pK = 5.5 and $N{\cdot}k_{off} = 1.0 \times 10^5\ s^{-1}$. These parameters for D_2O are pK = 6.0 and $N{\cdot}k_{off} = 3.0 \times 10^4\ s^{-1}$. Thus, there is a marked shift in the pK and the dissociation rate constant upon solvent substitution. The solutions contained 1 M NaCl, 2.5 mM of appropriate proton buffers, and the applied potential was +150 mV.

channel relative to the ionized state H^+A. The probabilities that the site is bound with a proton or not are:

$$p_{HA} = \tau_{HA}/(\tau_A + \tau_{HA}), \tag{3}$$

$$p_A = \tau_A/(\tau_A + \tau_{HA}), \tag{4}$$

where τ_A and τ_{HA} are the mean times spent in states A and H^+A, respectively. The mean time the site is occupied by a proton is given by $\tau_{HA} = 1/k_{off}$. Since it describes the residence time of the bound state, it depends on the strength of the interaction between the site and a proton, and is not a function of the proton concentration. On the contrary, the time $\tau_A = 1/(k_{on}[H^+])$, which is the mean time for a proton which reacts with the site to find it, is inversely proportional to the proton concentration because the collision frequency is proportional to $[H^+]$. The rate constant k_{on} relating the proton concentration and τ_A is defined by the accessibility of the site to a proton, which depends on the height of the potential barrier for association. The equilibrium constant K is defined by $K \equiv 10^{-pK} = k_{off}/k_{on}$. Thus

$$p_{HA} = 10^{pK-pH}/(1 + 10^{pK-pH}), \tag{5}$$

$$p_A = 1/(1 + 10^{pK-pH}). \tag{6}$$

For the two state system described in this way, the current spectral density can be written as (Machlup, 1954):

$$S_{pH}(f) = \frac{4\tau^2(\Delta i_1)^2}{(\tau_A + \tau_{HA})} \frac{1}{(1 + (2\pi f\tau)^2)}, \tag{7}$$

where Δi_1 is the difference in current between states A and H^+A, and τ is the relaxation time constant, which is defined by

$$\tau \equiv \tau_A\tau_{HA}/(\tau_A + \tau_{HA}). \tag{8}$$

To generalize this result for the multi-site model presented in Fig. 3, we note that contributions to the spectral density from N independent residues add, increasing the total value by a factor of N. On the other hand, the difference in current, Δi_1, in Eq. 7 is defined as $\Delta i_1 \equiv (\Delta i)/N$, where Δi is the total change in current through a completely ionized and deionized channel.

Thus, for N identical, independently ionizable sites, the spectral density is inversely proportional to N:

$$S_{pH}(f) = \frac{4(\Delta i)^2 10^{pK-pH}}{Nk_{off}(1 + 10^{pK-pH})^3} \frac{1}{(1 + (2\pi f\tau)^2)}. \tag{9}$$

In the low frequency limit ($f \Rightarrow 0$) the spectral density takes on the simple, frequency-independent form:

$$S_{pH}(0) = \frac{4(\Delta i)^2 10^{pK-pH}}{Nk_{off}(1 + 10^{pK-pH})^3}, \tag{10}$$

giving a maximum of the spectral density at pH ~ pK + 0.3.

Thus, by fitting the low frequency spectral density in Fig. 7 using a two parameter least-squares fit allows us to deduce $N{\cdot}k_{off}$ and the pK. The difference in current between the totally protonated and deprotonated states of the channel was measured directly from the single channel currents at pH 4.5 and 7.5 and is $\Delta i = 2.0 \times 10^{-11}$ A in 1 M NaCl in H_2O. The two parameter least-squares fit with $N{\cdot}k_{off} = 1.0 \times 10^5\ s^{-1}$ and pK = 5.5 is shown in Fig. 7 as the solid line. The agreement between the simple model illustrated by Fig. 3 and experiment is excellent. We discuss the results with D_2O later in this paper.

Using characteristic cutoff frequencies for measured spectra, we can determine the number of ionizable residues, N. In our model, the mean square value of the current fluctuations is inversely proportional to the number of sites. Indeed, large N corresponds to the superposition of many small events, which averages out the fluctuations. On the other hand, the mean square fluctuation is the product of the low frequency power spectral density $S_{pH}(0)$ and its bandwidth $f_c = (2\pi\tau)^{-1}$. In essence, Eq. 10 is a consequence of equating the ensemble and time averages of the current fluctuations. By rewriting Eq. 10 in terms of τ and solving for N, we have

$$N = 4\,(\Delta i)^2\,\tau\,10^{pK-pH}/[S_{pH}(0)(1 + 10^{pK-pH})^2], \tag{11}$$

where τ may be obtained from the inverse frequency at which the spectral density drops to one-half its low frequency value, $S(0)$ (see Eq. 1). For pH = 5.8, which corresponds to the maximum intensity of noise, an estimate of the relaxation time is $\tau = 3.1 \times 10^{-5}$ s (Fig. 4 *A*) and thus $N = 3.8$. Similar measurements performed for pH ~ 6.0 yield an average value of $N = 4.2 \pm 0.7$. Using the estimated value for the pK = 5.5, we find that the mean time a site is occupied with a proton is $\tau_{HA} = 4 \times 10^{-5}$ s. Since k_{off} is the inverse of τ_{HA}, $k_{off} = 2.5 \times 10^4\ s^{-1}$. Finally, we can also deduce a value for the association constant, k_{on}, since $k_{on} = k_{off}/K = 8 \times 10^9\ M^{-1}\ s^{-1}$. These

measurements completely characterize the dynamics of ionizable residue protonation.

The protonation reactions in the presence of H_2O are too rapid to determine a value for τ over a significant range of pH. Specifically, because the background noise spectral density at high frequency increases (see Fig. 4 *A*), our estimates of the cutoff frequency were restricted to values of pH = 5.8 ± 0.3. Using D_2O gave us an advantage here. In particular, the slowing down of the protonation dynamics caused by substituting H_2O with D_2O (compare Figs. 4 *B* and 5 *B*) enabled us to determine the cutoff frequency over a wider range of pH values. Fig. 8 shows the least-squares fits of a Lorentzian line (Eq. 1) to the spectral densities at three values of pD. To allow visualization of the fit to the data at high frequencies, the spectra shown in Fig. 8 are smoothed by averaging over a number, P_j, of nearest neighbor points. The number of points was increased with the frequency according to the algorithm $P_j = (j/50)$, where the index j ranges from 1 to 1024.

Fig. 9 illustrates the pD dependence of the relaxation time $\tau = (2\pi f_C)^{-1}$, where f_C is the corner frequency of the Lorentzian defined in Eq. 1. Note that the relaxation time increases as the pD is increased over the range 5.7 to 6.9 and saturates at higher pH values, which is predicted by the model presented in Fig. 3. From Eq. 8, it follows that the relaxation time approaches the value of the smaller time (τ_A or τ_{HA}) as the difference between these times increases.

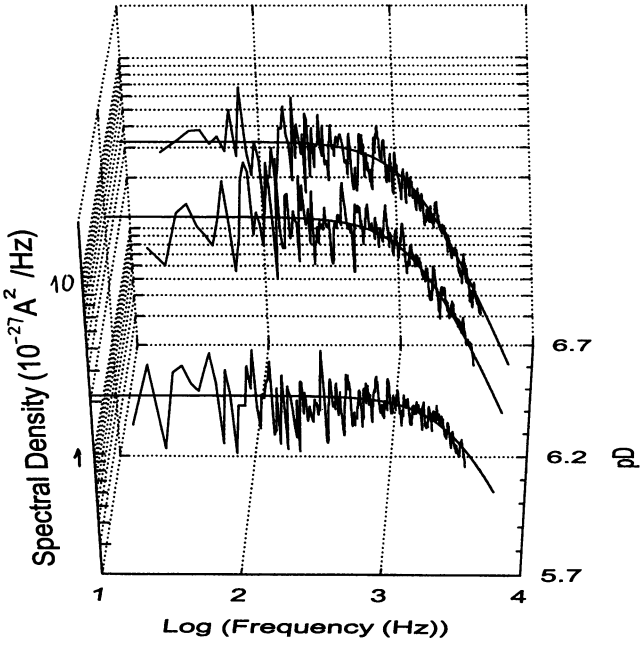

FIGURE 8 The spectral density as a function of pD and frequency. The decrease in the characteristic cutoff frequencies with increasing pD is clearly seen. Thus, the relaxation time for the interaction of D^+ with the channel residues is longer for lower bulk D^+ concentrations. The solid lines through the data are the least-squares, two parameter fit to a Lorentzian (Eq. 1), which is characteristic for a system with a single exponential relaxation. To allow visualization of the fit at high frequencies, the spectra were smoothed (see text). The solution contained 1 M NaCl in D_2O, and the applied potential was +150 mV.

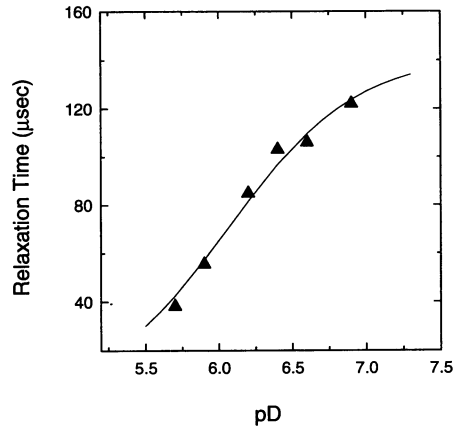

FIGURE 9 The pD dependence of the relaxation (correlation) time obtained from the fitting procedure outlined in Fig. 8. The relaxation time increases with pD and approaches a limiting value of $1/k_{off}$. The solid line illustrates the prediction of Eq. 12 with $\tau_{HA} = 1.5 \times 10^{-4}$ s and pK = 6.1. The latter parameter is in good agreement with that obtained independently from the low frequency spectral density amplitude data (Fig. 7). The solutions bathing the channel contained 1 M NaCl in D_2O.

Then, for high proton concentrations, the relaxation time is approximately equal to the time the site is unoccupied τ_A, which is relatively short and inversely proportional to the proton concentration. For the other limiting case, at low proton concentrations, the site is virtually always unoccupied, and the dwell time in the unoccupied state is much greater than that in the bound state. It means that the relaxation time τ is approximately equal to τ_{HA}, which is independent of pD.

The solid line through the points in Fig. 9 is a two parameter least-squares fit to Eq. 12

$$\tau = \tau_{HA}/(1 + 10^{pK-pH}) \qquad (12)$$

with pK = 6.1 and $\tau_{HA} = 1.5\ 10^{-4}$ s. This value of the pK is in good agreement with the value of 6.0 deduced from the low frequency spectral density (see Fig. 7). The rate constant for dissociation, $k_{off} = 6.7 \times 10^3\ s^{-1}$ was determined from the mean time a D^+ ion spends on a residue, since $k_{off} = 1/\tau_{HA}$.

As can be seen in Fig. 7, substitution of D_2O (Fig. 7, *open circles*) for H_2O (Fig. 7, *filled circles*) caused a marked shift in the pK of ~0.5. In addition, the amplitude of the low frequency noise increased by a factor of 2. A least-squares fit of Eq. 10 to the D_2O data with $\Delta i = 1.6 \times 10^{-11}$ A, which is illustrated by the dashed line, shows that the pK shifted from 5.5 (H_2O) to 6.0 (D_2O) and that $N \cdot k_{off}$ decreased from $1.0 \times 10^5\ s^{-1}$ to $3.0 \times 10^4\ s^{-1}$. Using the value of k_{off} from fitting the pD dependence of the relaxation times, we have $N = 4.6$. On the other hand, directly computing the number of residues from Eq. 11 with the pK value of 6.1 deduced from the least-squares fit shown in Fig. 9 and the data in Fig. 10 for +150 mV ($S(0) = 6.01 \times 10^{-27}$ A^2/Hz, $\tau = 1.02 \times 10^{-4}$ s, pD = 6.4), we obtain $N = 3.9$. Averaging the results of similar calculations for different pD values, we have $N = 4.1 \pm 0.6$.

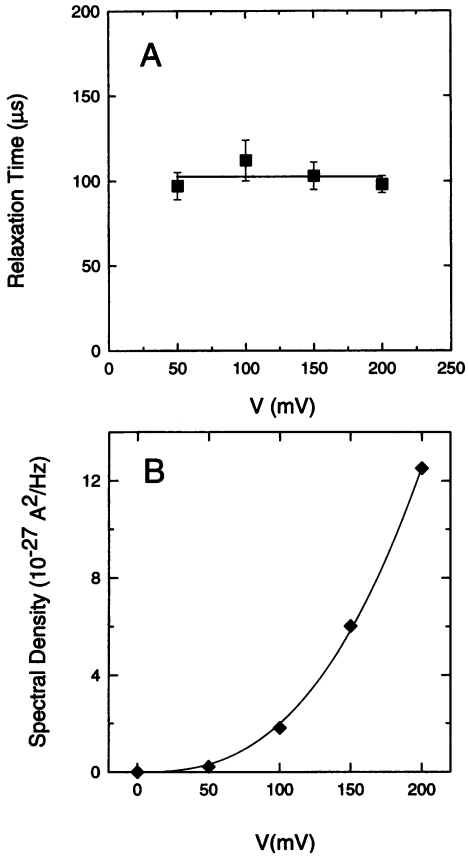

FIGURE 10 The voltage dependence of the noise provides strong evidence that the current fluctuations are generated by equilibrium ionization reactions. (*A*) The correlation time is independent of the applied potential. The solid line shows the average value of the relaxation times. (*B*) However, the low frequency spectral density is voltage dependent and proportional to $V^{2.7}$ indicating that the ionization induced conductance change is voltage sensitive. The solutions contained 1 M NaCl in D_2O and the pD = 6.4.

Fig. 10 *A* shows that the relaxation time of the protonation reaction is virtually unchanged by the applied potential over the range 50–200 mV. The deviation of any point from the average value (Fig. 10 *A*, *solid line*) is <10%. Note that the difference in energy to transfer an elementary charge through a membrane for 50 and 200 mV is ~6kT. Therefore, the pH-dependent noise reported here is essentially described by our equilibrium ionization model and is not caused by a field-induced ionization. It appears that protons are not driven by the applied potential to subsequently react with these ionizable residues.

For simple models of current noise generation by a linear circuit element with fluctuating conductance, one would expect a quadratic dependence of the low frequency spectral density on voltage (DeFelice, 1981). Fig. 10 *B* shows that for positive applied potentials, the noise varies as $V^{2.7}$. Thus, the relative contribution of ionization-controlled barriers to the channel conductance is voltage dependent. We are currently not in a position to speculate on possible mechanisms that could account for this particular dependence. Nevertheless, the model in Fig. 3 captures the essence of the protonation-induced noise, since for all positive applied potentials, only one ionization process with pK = 5.5 (H_2O) and pK = 6.0 (D_2O) was observed.

DISCUSSION AND CONCLUSIONS

A simple model based on a first order reaction describing the ionization of sites inside the channel accounts for our results. The magnitude of the pH-dependent noise exceeds by 100-fold (at pH 5.8 and pD 6.3) the shot noise expected for these currents. Protonation-induced conductance fluctuations are also much larger than possible contributions from anomalous electrolyte conductivity fluctuations related to high proton mobility (Bezrukov et al., 1989). According to our model, the channel conductance is modulated by the reversible charging of sites, which most likely induces changes in the electrostatic potential profile of the channel (see also Grigorjev and Bezrukov, 1994). The association rate constant, k_{on}, was assumed to be diffusion limited. Our estimates of the relaxation time constants show that the values for k_{on} are independent of the proton concentration, but change in a predictable direction upon substitution of H_2O by D_2O. The ratio of the association rate constants may be calculated from the ratio of the off rate constants and the pK shift, ΔpK = 0.5:

$$k_{on}^{H}/k_{on}^{D} = (k_{off}^{H}/k_{off}^{D})10^{-\Delta pK}, \quad (13)$$

giving a 1.2 reduction in the association rate constant. The ratio of the mobility of H^+ in H_2O to that of D^+ in D_2O is 1.43 (Kirshenbaum, 1951; Heiks et al., 1954).

It is well to note that since the reaction dynamics preclude resolution of individual conductance steps, we cannot test the validity of our simplifying assumption that each residue contributes equally to the total difference in current, Δi. Given the likelihood that these sites are close to each other, it is possible that they interact (see Fig. 6, Bezrukov and Kasianowicz, 1993). If they do interact, then it is conceivable that the magnitude of the current jump associated with the ionization of a particular site depends on the state of occupancy of the other $N - 1$ sites. If this is the case, it can be shown that the number of such sites estimated from our analysis would be different from the actual number of residues. We believe that the corrections, if any, will be small, especially since the experiments reported here were done in concentrated electrolyte solutions (1 M NaCl). Still, we hope that future experiments will enable us to determine whether a mean field approach (Tanford and Roxby, 1972) or a more detailed theory (Bashford and Karplus, 1991; Gilson and Honig, 1987), which could include interactions between sites, is sufficient to describe the ionization of neighboring residues inside this channel at lower electrolyte concentration.

Proton mobility near biological surfaces

Although it is known that protons play a central role in cellular bioenergetics (Mitchell, 1961; Nicholls, 1982), details of the mechanisms by which proton electrochemical gradients drive ATP synthetases are still elusive. Several alternative models to the chemiosmotic hypothesis have been suggested. Like Mitchell's scheme, some of these models assume that the pumping of protons across a membrane is required for ATP production. However, they further postulate that protons adjacent to a surface do not necessarily equilibrate with those in the bulk aqueous phase. In one scheme, a putative high resistance pathway to proton movement perpendicular to the membrane is assumed to retard proton flux to the bulk (e.g., Kell, 1979). Previous experimental evidence demonstrated that there is no such barrier (Kasianowicz et al., 1987b). Recent experiments with purple membrane fragments have been interpreted as evidence for this barrier (Scherrer et al., 1992; Heberle and Dencher, 1992; Heberle et al., 1994).

Other models in which protons are assumed to diffuse anomalously rapidly parallel to a membrane (Kell, 1979) or are somehow confined to the membrane surface (Haines, 1983) have been proposed. Teissie and co-workers sought to test this latter class of models by measuring the apparent proton diffusion coefficient over centimeter distances along lipid monolayers (Prats et al., 1986; but see Kasianowicz et al., 1987a). They claim that the diffusion coefficient of protons moving in the aqueous phase directly adjacent to the monolayer is ~20 times greater than that for protons in the bulk aqueous phase.

It is difficult to reconcile the latter result in light of experimental evidence to the contrary as reported here and elsewhere. Virtually all experiments on a variety of systems have shown that the effective diffusion coefficient for protons moving in close opposition to different types of biological surfaces or the rate constant for proton association to a group adsorbed to a surface is typically less than or equal to that for protons in the bulk aqueous phase. For example, Polle and Junge (1989) measured the rate at which the pH in the narrow aqueous spaces between stacked thylakoids relaxes after a light-induced pH jump. Also, Gutman and co-workers have studied extensively the dynamics of proton movement in many different environments (Gutman and Nachliel, 1990; Gutman et al., 1992a,b; Gutman et al., 1993). In these experiments, an increase in the H^+ activity is created with dye molecules that shift their pK upon illumination. The rapid spatial and temporal movement of protons is inferred from the relaxation of the fluorescence lifetime of a pH-dependent probe. Finally, pH-dependent fluorescent probes attached to well-defined sites on bacteriorhodopsin in purple membrane fragments suggest that the proton movement from the extracellular to the cytoplasmic side is not anomalously rapid (e.g., Heberle et al., 1994).

We observed protonation events that change the transport properties of the α-toxin pore in its fully functional state. Our estimate for k_{on} is similar to the diffusion-limited values measured by others for protonation reactions for free carboxyl or imidazole residues (Eigen et al., 1960, 1964; Eigen, 1964), which suggests that the state of water in this ion channel is similar to that in the bulk aqueous phase. It is interesting to note that despite the large disparity in time scales between our experimental method and that used by Gutman and colleagues, the conclusions we draw regarding protonation dynamics adjacent to the surfaces of biological molecules are essentially the same.

Comparison with other channels

Hess and colleagues reported that the dihydropyridine-sensitive Ca^{2+} channel exhibited pH-dependent gating (Pietrobon et al., 1988). Specifically, they showed that high proton concentrations lead to channel closure. (Interestingly, the value of k_{on} deduced from the experiments of Hess and colleagues is approximately an order of magnitude greater than the diffusion-limited rate constant for the reaction of protons with bases in water (Pietrobon et al., 1988; Prod'hom et al., 1987).) In this paper, we show that on a qualitative level, the gating properties of the α-toxin channel follow a similar pH-dependent gating pattern. As can be seen in Fig. 1, the probability that the α-toxin channel gates to the closed state increases when the pH decreases from 7.5 to 4.5. The results may suggest that either the relative energies of the open and closed states, or the potential barriers for a transition between these states, are pH sensitive. However, we did not address these questions here. Rather, we studied the physical cause of the pH-dependent current reduction in a fully open channel (Fig. 2). We estimated the number of current steps between the completely protonated and deprotonated states of the channel and the times characterizing the transitions between these states (Figs. 3 and 8, see discussion above). It should be noted that in contrast to the gating effect in both channels, the fully open α-toxin pore conductance increases with decreasing pH.

Recently, a cloned cyclic nucleotide-gated (CNG) channel was also shown to exhibit pH-dependent conductance changes (Root and MacKinnon, 1994). Histogram analysis and the sequential change in its single channel currents suggested that the proton binding sites of the CNG channel have identical pKs and are non-interacting, as was previously proposed for the α-toxin channel (Bezrukov and Kasianowicz, 1993). It is interesting that in contrast to the pH dependence of the current through single α-toxin channels, the conductance in the CNG channel decreases when the pH is lowered. Earlier, evidence was presented suggesting that pH-induced conductance changes, at least in the case of the α-toxin channel, are the direct consequence of an electric field effect and not related to structural changes (Bezrukov and Kasianowicz, 1993). A similar conclusion was tentatively reached for the CNG channel (Root and MacKinnon, 1994).

To determine the mobility of protons in the lumen of an ion channel, Gutman and colleagues measured the fluores-

cence relaxation of pyranine bound to the phoE protein in aqueous solution (Gutman et al., 1992b). Based on the assumption that the dye was bound to the center of the channel lumen, they concluded that the proton diffusion coefficient is reduced by 50% with respect to that of bulk water. However, it should be stressed that the precise location of the chromophore-binding site was inferred from the fluorescence lifetime data themselves. Besides, although this channel is comprised of three monomers embedded in a lipid bilayer (Jap, 1989), the conformation of the protein complex in aqueous solution may be different.

Nature of the binding sites

Since the effective pK of the groups that cause pH-dependent current noise in the α-toxin channel is 5.5 for positive applied potentials, we are tempted to speculate that the amino acids responsible for the effect are either histidines (pK = 6.1), glutamic acids (pK = 4.3), or aspartic acids (pK = 3.9). However, chemical modification of the α-toxin channel led Menestrina and colleagues (Cescatti et al., 1991) to conclude that the residues controlling the pH-dependent *I-V* relationship are lysines (pK = 10.5). It is well to note that there are reports of significant environment-dependent pK shifts for ionizable fluorescent probes (Chattopadhyay and London, 1988) and for amino acids. For example, the pK of histidines in several proteins were shown to range from 5.4 (Cohen et al., 1970) to 8 (Rüterjans and Pongs, 1971). Even larger shifts are realized when glutamic acids are placed in an extremely hydrophobic environment (Urry et al., 1992). In this case, it is natural to expect a pronounced change in the on and/or off rate constants from those measured for ionizable groups in water. It is hoped that site-directed mutagenesis coupled with measurements of pH-induced current noise will identify or exclude which site or sites are the cause of the pH-dependent current modulation in this channel.

Shift in pK values caused by solvent substitution

Studies of the effects of D_2O/H_2O solvent substitution on the pKs of some ionizable amino acids show that for short oligopeptides, the pK shifts by ~0.4–0.5 pH units (Bundi and Wüthrich, 1979). Similar findings were reported for globular proteins (Kalinichenko and Lobyshev, 1976) and are consistent with the 0.5 pH unit shift we observe in the pH (pD) dependence of the current noise. However, Goto et al. (1993) found no D_2O/H_2O-induced pK shift in the pH-dependent folding/unfolding transitions of cytochrome *c*. Specifically, after correcting the pD value as measured with a pH glass electrode, they showed that the titration of cytochrome *c* in D_2O is very similar to that in H_2O.

Structural implications

For the past 25 years, it was assumed by others that the channel formed by α-toxin was a hexamer (Bhakdi et al., 1981; Tobkes et al., 1985; Olofsson et al., 1988). However, recent gel-shift electrophoresis experiments offer compelling evidence that α-toxin adsorbed onto rabbit erythrocytes forms heptameric complexes that are believed to form the pore (Gouaux et al., 1994). These results and our analysis suggest there is at most one site per monomer that elicits the pH-induced current noise reported here.

Ionization noise as a structural probe

Given the difficulty of obtaining and interpreting high resolution crystal data for membrane-bound proteins, new methods of characterizing the structures of such macromolecules are needed. To correlate channel structure and function, genetic engineering was coupled to measurements of the steady state conductance and selectivity of the voltage-dependent ion channel (VDAC) (Blachly-Dyson et al., 1990). We hope that the analysis of ionization-induced current noise combined with site-directed mutagenesis and subsequent targeted chemical modification (Bayley, 1994) will serve as a useful tool to probe the functional structure of ion channels.

In addition to determining ion channel functional structure, there are also technological aspects that might be addressed with our technique. For example, a thorough characterization of the residues that line α-toxin channel lumen, or that of other large pores, might aid the rational design of genetically engineered mutants with novel properties. Strategic design of α-toxin mutants has already resulted in the design of pores that can be gated by enzymes (Walker and Bayley, 1994) and by metal ions (Walker et al., 1994).

We thank Drs. V. A. Parsegian, I. Vodyanoy, B. Robertson, and H. Bayley for constructive comments on the manuscript.

Supported in part by a National Academy of Sciences/National Research Council Research Associateship (J. J. K.), and by a grant from the Office of Naval Research (to V. A. Parsegian). The α-toxin sample was a generous gift from Dr. H. Bayley.

REFERENCES

Bashford, D., and M. Karplus. 1991. Multiple site titration curves of proteins: an analysis of exact and approximate methods and their calculation. *J. Phys. Chem.* 95:9556–9561.

Bates, R. G. 1973. Determination of pH. Theory and Practice. John Wiley & Sons, New York.

Bayley, H. 1994. Triggers and switches in a self-assembling pore-forming protein. *J. Cell. Biochem.* 56:177–182.

Bean, R. C., W. C. Shepard, H. Chen, and J. Eichner. 1969. Discrete conductance fluctuations in lipid bilayer protein membranes. *J. Gen. Physiol.* 53:741–757.

Bezrukov, S. M., and J. J. Kasianowicz. 1993. Current noise reveals protonation kinetics and number of ionizable sites in an open protein ion channel. *Phys. Rev. Lett.* 70:2352–2355.

Bezrukov, S. M., M. A. Pustovoit, A. I. Sibilev, and G. M. Drabkin. 1989. Large-scale conductance fluctuations in solutions of strong electrolytes. *Physica B (North-Holland).* 159:388–398.

Bhakdi, S., R Füssle, and J. Tranum-Jensen. 1981. Staphylococcal α-toxin: oligomerization of hydrophilic monomers to form amphiphilic hexamers

induced through contact with deoxycholate detergent micelles. *Proc. Natl. Acad. Sci. USA.* 78:5475–5479.

Bhakdi, S., M. Muhly, and R. Füssle. 1984. Correlation between toxin binding and hemolytic activity in membrane damage by staphylococcal α-toxin. *Infect. Immun.* 46:318–323.

Bhakdi, S., and J. Tranum-Jensen. 1991. α-Toxin of *Staphylococcus aureus. Microbiol. Rev.* 55:733–751.

Blachly-Dyson, E., S. Z. Peng, M. Colombini, and M. Forte. 1990 Alteration of the selectivity of the VDAC ion channel by site directed mutagenesis. *Science.* 247:1233–1236.

Bundi, A. and K. Wüthrich. 1979. 1H-NMR parameters of the common amino acid residues measured in aqueous solutions of the linear tetrapeptide H-Gly-Gly-X-L-Ala-OH. *Biopolymers.* 18:285.

Cescatti, L., C. Pederzolli, and G. Menestrina. 1991. Modification of lysine residues of *Staphylococcus aureus* α-toxin: effects on its channel forming properties. *J. Membr. Biol.* 119: 53–54.

Chattopadhyay, A., and E. London. 1988. Spectroscopic and ionization properties of *N*-(7-nitrobenz-2-oxa-1,3-diazol-4-yl)-labeled lipids in model membranes. *Biochim. Biophys. Acta.* 938:24–34.

Cohen, J. S., R. Shrager, M. McNeel, and A. N. Schnechter. 1970. On-line computer-assisted analysis of 220 MHz NMR data of protein imidazole resonances. *Biochim. Biophys. Res. Commun.* 40:144–151.

Covington, A. K., M. Paabo, R. A. Robinson, and R. G. Bates. 1968. Use of the glass electrode in deuterium oxide and the relation between the standardized pD (pa_0) scale and the operational pH in heavy water. *Anal. Chem.* 40:700–706.

Deamer, D. W. 1992. Role of water in proton flux mechanisms. *In* Biomembrane Structure and Function. The State of the Art. B. P. Gaber and K. R. K. Eswaren, editors. Adenine Press, Schenectady, NY. 209–226.

Deamer, D. W., and J. W. Nicholls. 1989. Proton flux in model and biological membranes. *J. Membr. Biol.* 107:91–103.

DeFelice, L. J. 1981. Introduction to Membrane Noise. Plenum Press, New York.

Eigen, M. 1964. Proton transfer, acid-base catalysis, and enzymatic hydrolysis. I. Elementary processes. *Ange. Chem. Int. Ed. Engl.* 3:1–72.

Eigen, M., G. G. Hammes, and K. Kustin. 1960. Fast reactions of imidazole studied with relaxation spectrometry. *J. Am. Chem. Soc.* 82:3482–3483.

Eigen, M., W. Kruse, G. Maas, and L. DeMaeyer. 1964. Rate constants of proteolytic reactions in aqueous solutions. *Prog.. React. Kinet.* 2:287–318.

Fishman, H. M., and H. R. Leuchtag. 1990. Electrical noise in physics and biology. *In* Current Topics in Membranes and Transport. 37:3–35.

Füssle, R., S. Bhakdi, A. Sziegoleit, J. Tranum-Jensen, T. Kranz, and H.-J. Wellensiek. 1981. *J. Cell Biol.* 91:83–94.

Gardiner, C. W. 1985. Handbook of Stochastic Methods for Physics, Chemistry and the Natural Sciences, 2nd ed. Springer-Verlag, New York.

Gilson, M. K., and B. H. Honig. 1987. Calculation of electrostatic potentials in an enzyme active site. *Nature (Lond).* 330:84–86.

Glasoe, P. K., and F. A. Long. 1960. Use of glass electrodes to measure acidities in deuterium oxide. *J. Phys. Chem.* 64:188–190.

Goto, Y., Y. Hagihara, D. Hamada, M. Hoshino, and I. Nishii. 1993. Acid-induced unfolding and refolding transitions of cytochrome *c*: a three-state mechanism in H_2O and D_2O. *Biochemistry.* 32: 11878–11885.

Gouaux, J. E., O. Braha, M. R. Hobaugh, L. Song, S. Cheley, C. Shustak, and H. Bayley. 1994. Subunit stoichiometry of staphylococcal α-hemolysin in crystals and on membranes: a heptomeric pore. *Proc. Natl. Acad. Sci. USA.* 91:12828–12831.

Gray, G. S., and M. Kehoe. 1984. Primary sequence of the α-toxin gene from *Staphylococcus aureus* Wood 46. *Infect. Immun.* 46:615–618.

Grigorjev, P. A., and S. M. Bezrukov. 1994. Hofmeister effect in ion transport: reversible binding of halide anions to the roflamycoin channel. *Biophys. J.* 67:2265–2271.

Gutman, M., A. B. Kotlyar, N. Borovok, and E. Nachliel. 1993. Reaction of bulk protons with a mitochondrial inner membrane preparation: time-resolved measurements and their analysis. *Biochemistry.* 32: 2942–2946.

Gutman, M., and E. Nachliel. 1990. The dynamic aspects of proton transfer processes. *Biochim. Biophys. Acta.* 1015:391–414.

Gutman, M., E. Nachliel, and S. Kiryati. 1992a. Dynamic studies of proton diffusion in mesoscopic heterogeneous matrix. II. The interbilayer space between phospholipid membranes. *Biophys. J.* 63:281–290.

Gutman, M., Y. Tsfadia, A. Masad, and E. Nachliel. 1992b. Quantitation of physical-chemical properties of the aqueous phase inside the phoE ionic channel. *Biochim. Biophys. Acta.* 1109:141–148.

Haines, T. H. 1983. Anionic lipid headgroups as a proton-conducting pathway along the surface of membranes: a hypothesis. *Proc. Natl. Acad. Sci. USA.* 80:160–164.

Heberle, J., and N. A. Dencher. 1992. Surface-bound optical probes monitor proton translocation and surface potential changes during the bacteriorhodopsin photocycle. *Proc. Natl. Acad. Sci. USA.* 89:5996–6000.

Heberle, J., J. Riesle, G. Thiedemann, D. Oesterhelt, and N. A. Dencher. 1994. Proton migration along the membrane surface and retarded surface to bulk transfer. *Nature.* 370:379–382.

Heiks, J. R., M. K. Barnett, L. V. Jones, and E. Orban. 1954. The density, surface tension and viscosity of deuterium oxide at elevated temperatures. *J. Phys. Chem.* 58:488–491.

Heinemann, S. H., and F. J. Sigworth. 1991. Open channel noise. V. Fluctuating barriers to ion entry in gramicidin A channels. *Biophys. J.* 57:49–514.

Hille, B. 1992. Ionic Channels of Excitable Membranes, 2nd ed. Sinauer Associates, Inc., Sunderland, MA.

Ikigai, H., and T. Nakae. 1987. Assembly of the α-toxin-hexamer of *Staphylococcus aureus* α-toxin in the liposome membrane. *J. Biol. Chem.* 262:2156–2160.

Jap, B. K. 1989. Molecular design of PhoE porin and its functional consequences. *J. Mol. Biol.* 205:407–419.

Kalinichenko, L. P., and V. P. Lobyshev. 1976. Should the pH = pD condition be used in biological experiments with heavy water as a solvent? *Stud. Biophys.* 58:235–240.

Kasianowicz, J., R. Benz, M. Gutman, and S. McLaughlin. 1987a. Reply to: Lateral diffusion of protons along phospholipid monolayers. *J. Membr. Biol.* 99:227.

Kasianowicz, J., R. Benz, and S. McLaughlin. 1987b. How do protons cross the membrane-solution interface? Kinetic studies on bilayer membranes exposed to the protonophore S-13 (5-chloro-3-tert-butyl-2′-chloro-4′nitrosalicylanilide). *J. Membr. Biol.* 95:73–89.

Kell, D. B. 1979. On the functional proton current pathway of electron transport of phosphorylation. An electrodic view. *Biochim. Biophys. Acta.* 549:55–99.

Kirshenbaum, I., editor. 1951. Physical Properties and Analysis of Heavy Water. McGraw-Hill, New York.

Krasilnikov, O., R. Z. Sabirov, V. I. Ternovsky, P. G. Merzliak, and J. N. Murathojaev. 1992. A simple method for the determination of the pore radius of ion channels in planar lipid bilayer membranes. *FEMS Microbiol. Immunol.* 105:93–100.

Machlup, S. 1954. Noise in semiconductors: spectrum of a two-parameter random signal. *J. Appl. Physics* 25:341–343.

Menestrina, G. 1986. Ionic channels formed by *Staphylococcus aureus* α-toxin: voltage-dependent inhibition by divalent and trivalent cations. *J. Membr. Biol.* 90:177–190.

Mitchell, P. 1961. Coupling of phosphorylation to electron and hydrogen transfer by a chemiosmotic type of mechanism. *Nature (Lond).* 191: 144–148.

Montal, M., and P. Mueller. 1972. Formation of bimolecular membranes from lipid monolayers and study of their properties. *Proc. Natl. Acad. Sci. USA.* 65:3561–3566.

Neher, E., and B. Sakmann. 1976. Single channel currents recorded from membrane of denervated frog muscle fibers. *Nature (Lond).* 260: 799–802.

Neumcke, B. 1982. Fluctuation of Na and K currents in excitable membranes. *Int. Rev. Neurobiol.* 23:35–67.

Nicholls, D. G. 1982. Bioenergetics. An Introduction to the Chemiosmotic Theory. Academic Press, New York.

Olofsson, A., U. Kaveus, M. Thelestam, and H. Hebert. 1988. The projection structure of α-toxin from *Staphylococcus aureus* in human platelet

membranes as analyzed by electron microscopy and image processing. *J. Ultrastruct. Mol. Struct. Res.* 100:194–200.

Palmer, M., R. Jursch, U. Weller, A. Valeva, K. Hilgert, M. Kehoe, and S. Bhakdi. 1993. *Staphylococcus aureus* α-toxin. Production of functionally intact, site-specifically modifiable protein by introduction of cysteine at positions 69, 130, and 186. *J. Biol. Chem.* 268:11959–11962.

Pietrobon, D., B. Prod'hom, and P. Hess. 1988. Conformational changes associated with ion permeation in L-type calcium channels. *Nature (Lond).* 333:373–376.

Polle, A., and W. Junge. 1989. Proton diffusion along the membrane surface of thylakoids is not enhanced over that in bulk water. *Biophys. J.* 56:27–31.

Prats, M., J. Teissie, and J.-F. Tocanne. 1986. Lateral proton conduction at lipid water interfaces and its implications for the chemiosmotic hypothesis. *Nature (Lond).* 322:756–758.

Prod'hom, B., D. Pietrobon, and P. Hess. 1987. Direct measurement of proton transfer rates to a group controlling the dihydropyridine-sensitive Ca^{2+} channel. *Nature (Lond).* 329:243–246.

Root, M. J., and R. MacKinnon. 1994. Two identical noninteracting sites in an ion channel revealed by proton transfer. *Science.* 265:1852–1856

Rüterjans, H., and O. Pongs. 1971. On the mechanism of action of ribonclease T1 nuclear magnetic resonance study on the active site. *Eur. J. Biochem.* 18:313–318.

Scherrer, P., U. Alexiev, J. Otto, M. P. Heyn, T. Marti, and G. H. Khorana. 1992. Proton movement and surface charge in bacteriorhodopsin detected by selectively attached pH indicators. *In* Structures and Functions of Retinal Proteins. J. Rigaud, editor. Colloque Inserm, John Libbey Eurotext Ltd. 221:205–211.

Schottky, W. 1918. Über spontane stromschwankungen in verschiedenen elektrizitätleitern. *Ann. der Physik.* 57:541–567.

Sigworth, F. J. 1985. Open channel noise. I. Noise in acetylcholine receptor currents suggest conformational fluctuations. *Biophys. J.* 47:709–720.

Stanley, H. E. 1971. Introduction to Phase Transitions and Critical Phenomena. Oxford University Press, New York.

Stevens, C. F. 1977. Study of membrane permeability changes by fluctuation analysis. *Nature (Lond).* 270:391–396.

Swain, C. G., and D. F. Evans. 1966. Conductance of ions in light and heavy water at 25°. *J. Am. Chem. Soc.* 88:383–390.

Tanford, C., and R. Roxby. 1972. Interpretation of protein titration curves. Application to lysozyme. *Biochemistry.* 11:2192–2198.

Thelestam, M., and M. Blomqvist. 1988. Staphylococcal α-toxin: recent advances. *Toxicon.* 26:51–65.

Tobkes, N., B. A. Wallace, and H. Bayley. 1985. Secondary structure and assembly mechanism of an oligomeric channel protein. *Biochemistry.* 24:1915–1920.

Urry, D. W., D. C. Gowda, S. Q. Peng, T. M. Parker, and R. D. Harris. 1992. Design at nanometric dimensions to enhance hydrophobicity-induced pK_a shifts. *J. Am. Chem. Soc.* 114:8716–8717.

van Kampen, N. G. 1981. Stochastic Processes in Physics and Chemistry. North-Holland, New York.

Walker, B., and H. Bayley. 1994. A pore-forming protein with a protease activated trigger. *Protein Eng.* 7:91–97.

Walker, B., J. Kasianowicz, M. Krishnasastry, and H. Bayley. 1994. A pore-forming protein with a metal-actuated switch. *Protein Eng.* 7:655–662.

Walker, B., M. Krishnasastry, L. Zorn, J. Kasianowicz, and H. Bayley. 1992. Functional expression of the α-hemolysin of *Staphylococcus aureus* in intact *Escherichia coli* and in cell lysates. *J. Biol. Chem.* 267:10902–10909.

Wax, N., editor. 1954. Selected Papers on Noise and Stochastic Processes. Dover, New York.